Oligonucleotide and Water Self-Diffusion in Systems of Pluronic Triblock Copolymers and in Buffer Solutions by Pulsed Field Gradient Nuclear Magnetic Resonance

Darren A. Hadden,[†] Randolph L. Rill,[‡] Lori McFaddan,[§] and Bruce R. Locke*[,†]

Department of Chemical Engineering, Florida State University and Florida A & M University, FAMU-FSU College of Engineering, and Department of Chemistry and Department of Biological Sciences, Florida State University, Tallahassee, Florida 32310-6046

Received September 3, 1999; Revised Manuscript Received January 18, 2000

ABSTRACT: Pulsed field gradient nuclear magnetic resonance (PFGNMR) measurements of oligonucleotide (poly-thymidine, T_1 to T_{30}) self-diffusion coefficients in gels of Pluronic [poly(ethylene oxide) (PEO)−poly(propylene oxide) (PPO)−poly(ethylene oxide) (PEO)] micelles follow the Zimm scaling theory that predicts the diffusion coefficient to vary with solute molecular weight to the −0.5 power. The ratio of the diffusion coefficients in a 20% Pluronic gel-like liquid crystal phase to those in buffer solutions (without Pluronics) was approximately equal to 0.5 for all molecule sizes tested. PFGNMR water self-diffusion coefficient measurements in the gel phase and the solution phase of Pluronic micelles were interpreted within the context of volume averaging theory and known structural features of Pluronic micelles for various Pluronic concentrations. The result of combining the volume averaging theory and measurements of water and oligonucleotide self-diffusion indicates that the geometrical constraints of the Pluronic structure are sufficient to explain the majority of the oligonucleotide self-diffusion coefficient reduction in the Pluronic gel-like system.

Introduction

Triblock copolymers made of chains of poly(ethylene oxide) (PEO) and poly(propylene oxide) (PPO) subunits are currently subjects of intensive interest and research due to their potential as support media for capillary electrophoresis[1−6] as well as their many other uses (see for example ref 7). Chains of $(PEO)_x(PPO)_y(PEO)_x$ are commercially available with a wide range of subunit compositions and go under the trade name of Pluronic. Because of the physical-chemical nature of the oxide subunits, single chains of these molecules will associate to form micelles with the more hydrophobic PPO units packed within a core surrounded by the more hydrophilic PEO units. Extensive studies have been conducted to determine the phase behavior of a variety of triblock formulations as functions of temperature and polymer concentration in aqueous solutions.[8−11] Light scattering methods,[12,13] small-angle neutron scattering,[14,15] rheological methods,[14,16] transmission electron microscopy,[15] scanning calorimetry,[16] and NMR water self-diffusion[17] have been applied to determine the basic structural features of Pluronic micelles, and the general view is that the micelles will pack in a cubic lattice[2,18] to form a gel-like medium under well-defined conditions of concentration and temperature.

F-127, i.e., $(PEO)_{100}(PPO)_{70}(PEO)_{100}$, will form a gel-like phase of associated individual micelles at room temperature and at a concentration of about 20%. Under these conditions the hydrophobic core, consisting of PPO subunits, is approximately 9 nm in diameter and is surrounded by a region of PEO to give an overall micelle diameter of approximately 18 nm.[3,9] This medium has been shown to be effective for the separation of a wide range of macromolecules including double-stranded DNA up to 3000 base pairs by conventional electrophoresis[3] and single-stranded DNA from 4 to 60 nucleotides long and oligonucleotides (e.g., polythymidines) of 12−24 nucleotides long by capillary electrophoresis.[3,6] These results are very interesting not only for their practical utility but also for the implications on fundamental aspects of macromolecular transport in complex porous media.

The structures of these gel-like systems of micelles are very different from conventional electrophoresis media made from chemically and physically cross-linked polymers of polyacrylamide and agarose.[19] The absence of chemical or physical cross-links in the Pluronic gel-like phases may allow a larger degree of freedom for macromolecular transport around the obstacles that make up the medium than occurs in conventional electrophoresis media. For example, the electrophoretic mobility of DNA from 100 to 1800 base pairs was larger in Pluronic than could be accounted for by reptation theory which predicts the electrophoretic mobility to be inversely proportional to the length of the macromolecule.[3] Furthermore, the electrophoretic mobility of the oligonucleotides (T_{12}−T_{18}) varied with molecular weight as $M^{-0.36}$ in a 20% gel.[20] Electrophoresis studies provide information on molecular transport in the presence of an applied force; however, a full understanding of molecular transport in porous media also requires knowledge of diffusive motion.

Diffusion of macromolecules in polymer gels and solutions has been extensively studied both experimentally and theoretically.[21−23] The major factors that affect diffusion of macromolecules in polymer gels and solutions include such molecular properties as size and shape, such media properties as geometry and obstacle concentration, and hydrodynamic and physical-chemical interactions between the diffusing solute and the back-

[†] Department of Chemical Engineering, FAMU-FSU.
[‡] Department of Chemistry, FSU.
[§] Department of Biological Sciences, FSU.
* Corresponding author: Tel 850-410-6165; FAX 850-410-6150; E-mail locke@eng.fsu.edu.

10.1021/ma9915071 CCC: $19.00
Published on Web 04/29/2000

ground matrix. In addition to the classic Rouse,[24] Zimm,[25] and reptation theories[26,27] to describe the effects of polymer length on macromolecular diffusion, many other approaches[28−36] have been used to describe the effects of molecular size, media structure, and concentration of obstacles. The nature of how the diffusion of macromolecules scale with molecular size and media geometry in systems of Pluronic micelles is not known.

The present study therefore considers the diffusion of oligonucleotides as a function of chain length from T_1 to T_{30} in 20% Pluronic F-127 gel-like phases. Pulsed field gradient nuclear magnetic resonance (PFGNMR) is used to measure oligonucleotide self-diffusion in the liquid crystal phase of Pluronic and, for comparison, in buffer solutions without Pluronic. The results are interpreted within the context of well-established theories of macromolecular diffusion in polymer solutions and gels. In addition, water self-diffusion results, obtained in the present work and from the literature,[17] are analyzed within the context of volume averaging theory[37] to describe the effects of media geometry on effective diffusion coefficients of small solutes. Finally, results from the water and oligonucleotide self-diffusion measurements and volume averaging theory are combined to show that the major restriction to diffusion of oligonucleotide molecules with sizes up to 30 nucleotides is the geometrical constraints of the Pluronic micelles.

Materials and Methods

Thymidine monophosphate (T_1) was obtained from Sigma Chemical Co. (St. Louis, MO), and oligonucleotides T_3, T_5, T_{10}, T_{20}, and T_{30} were synthesized at the Biochemical Analysis and Synthesis Service (BASS) Lab in the Department of Chemistry at Florida State University. Stock solutions of 89 mM Tris base, 89 mM boric acid, and 2 mM EDTA (TBE) were prepared with 2 mM cacodylic acid to prevent microorganism growth. The oligonucleotides were dissolved in 1X TBE stock solution to make approximately 110 mM solutions based on total thymidine monophosphate. The final concentrations were measured by UV spectroscopy and ranged from 103 to 113 mM. The samples were then heated in a 90 °C water bath for 7 min to separate any aggregated oligonucleotides. Approximately 300 μL of each sample was added to 5 mm diameter NMR tubes for diffusion measurements in solution.

Pluronic F127 (BASF Performance Chemicals, Mt. Olive, NJ) was prepared in 20% concentrations (grams of Pluronic per 100 mL of solution). The Pluronic was added to the buffer solution in the cold room at 4−5 °C and agitated for approximately 24 h or until the Pluronic was dissolved in the solution. The samples were then microcentrifuged for about 1 h to remove air. The samples were brought to room temperature (22−24 °C) at which point they transformed into the liquid crystalline phase. Samples of the six different lengths of oligonucleotides (T_1, T_3, T_5, T_{10}, T_{20}, and T_{30}) were prepared in both buffer solution (without Pluronic) and Pluronic gels (containing buffer), giving a total of 12 samples. At least three diffusion experiments were performed on each sample.

The Pluronic used in the present study, F-127, has a composition, as specified by the manufacturer, of $(PEO)_{100}$-$(PPO)_{70}(PEO)_{100}$. All experiments were performed with samples from the same lot. There are minor lot-to-lot variations in the overall composition.

The sample preparation method for the water self-diffusion measurements was identical to the method described above with the omission of the oligonucleotides, the cacodylic acid, and the heating step. Water diffusion measurements were made at Pluronic concentrations of 0%, 10%, 15%, 20%, 25%, and 30% (grams Pluronic/100 mL of solution). Three different samples were made for each concentration, and then three diffusion measurements were made on each sample.

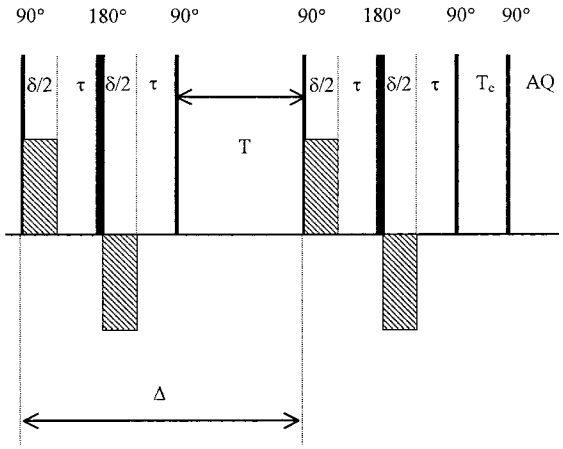

Figure 1. BPLED pulsing diagram for NMR experiments.

Diffusion measurements were based on the Hahn[38] spin-echo sequence and later modifications by Car and Purcell,[39] the pulsed field gradient nuclear magnetic resonance method (PFGNMR) by Stejskal and Tanner,[40] and stimulated echoes as introduced by Tanner.[41] The particular sequence used in the present study is the bipolar pulse pair (BPP) longitudinal eddy-current delay (LED) stimulated-echo sequence[42,43] as shown in Figure 1. In the absence of convective flow, the amplitudes of the free induction decay (FID) after the fifth 90° pulse are given by

$$S(q) = S(0)\exp\left[-Dq^2\left(\Delta - \frac{\delta}{3} - \frac{\tau}{2}\right)\right] \quad (1)$$

where $q = \gamma g\delta$, γ is the magnetogyric ratio of the nucleus, g is the gradient amplitude, and δ is the gradient pulse duration. For a given experiment, all the parameters in eq 1 are known except for the diffusion coefficient D. The echo attenuation data was fit to eq 1 using a weighted least-squares regression, and the R^2 values ranged from 0.854 to 0.995 with only 8 of 48 data sets with R^2 below 0.900.

All the experiments were performed on a Bruker 270 MHz NMR spectrometer with a Techron gradient system located in the Magnetic Resonance Facility in the Department of Chemistry of the Florida State University, Tallahassee, FL. The probes used were built in-house and were equipped with saddle rf coils and gradient capability.

The probe for the oligonucleotide measurements held a 5 mm NMR tube vertically and was tunable to both ^{1}H and ^{31}P. The gradients were calibrated using the BPP-LED sequence with deionized water, and the method was checked by measuring the diffusion coefficient of a known compound, phosphocreatine. Diffusion measurements of the oligonucleotides were made using the nucleus ^{31}P. Referring to the sequence in Figure 1, T was 10 ms, τ was 75 μs, and T_e was 10.05 ms for all experiments. The timing parameters Δ and δ were varied from 12.7 to 15.9 ms and 2.2 to 5.4 ms, respectively. In addition, for each experiment, five gradient values were used: 48.7, 67.1, 85.5, 103.8, and 122.2 G/cm. The data were fit directly to eq 1 in order to calculate the diffusion coefficients.

The probe for the water diffusion measurements also had a dual-tune ^{31}P and ^{1}H solenoid coil with gradient capability and was used to detect protons. In this case, the samples were held horizontally in disposable 100 μL capillary tubes. The BPP-LED pulse sequence was used with parameter values of $\gamma = 2.67512 \times 10^4$ s^{-1} G^{-1}, $\delta = 50$ μs, $\Delta = 0.049$ s, and $\tau = 25$ μs. The gradient values were varied from 253 to 507 G/cm. The amplitudes of the free induction decays were measured as functions of the above parameters, and the effective water diffusion coefficients were calculated according to eq 1.

Volume Averaging Theory

The method of volume averaging provides a means to describe transport in a multiphase system using

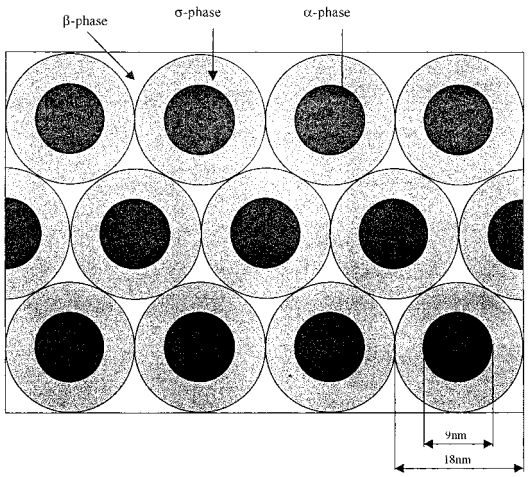

Figure 2. Two-dimensional view of Pluronic copolymer liquid crystals. The central black regions (α phase) represent the hard cores consisting of the hydrophobic poly(propylene oxide). The dark gray regions (σ phase) represent the hydrated poly(ethylene oxide). The light regions (β phase) represent the interstitial aqueous phase. This diagram illustrates 22 wt % Pluronic F127 (after refs 4 and 9).

information on transport in single-phase systems and the geometry of the multiphase system.[37,44] The Pluronic system consists of three different phases, shown in Figure 2(and Figure A1), that include the hydrophobic PPO cores (α phase), the hydrated PEO regions (σ phase), and the interstitial aqueous phase (β phase). The species material balances for a small solute in the σ and β phases, neglecting convective transport and chemical reaction, are

$$\frac{\partial C_\sigma}{\partial t} = \vec{\nabla}\cdot(D_\sigma \vec{\nabla} C_\sigma) \quad \text{in } V_\sigma \tag{2}$$

$$\frac{\partial C_\beta}{\partial t} = \vec{\nabla}\cdot(D_\beta \vec{\nabla} C_\beta) \quad \text{in } V_\beta \tag{3}$$

and no equation is needed for the α phase since it is impermeable to hydrophilic solutes. C_β and C_σ represent the local point concentrations of the solute in the β and σ phases, respectively. V_β and V_σ are the averaging volumes for the two phases.[37] The boundary conditions are

$$\text{BC 1:} \quad -\hat{n}_{\beta\sigma}\cdot D_\beta \vec{\nabla} C_\beta = -\hat{n}_{\beta\sigma}\cdot D_\sigma \vec{\nabla} C_\sigma \quad \text{at } A_{\beta\sigma} \tag{4}$$

$$\text{BC 2:} \quad -\hat{n}_{\sigma\beta}\cdot D_\sigma \vec{\nabla} C_\sigma = P(C_\sigma - K_{eq} C_\beta) \quad \text{at } A_{\beta\sigma} \tag{5}$$

$$\text{BC 3:} \quad \hat{n}_{\alpha\sigma}\cdot D_\sigma \vec{\nabla} C_\sigma = 0 \quad \text{at } A_{\alpha\sigma} \tag{6}$$

The first boundary condition is a statement of equality of fluxes at the interface between the β and σ phases, $A_{\beta\sigma}$. The second boundary condition defines the same flux in terms of a mass-transfer coefficient and an equilibrium partitioning coefficient K_{eq}. In the limit where P goes to infinity, this boundary condition becomes a linear equilibrium boundary condition of the form $C_\sigma = K_{eq} C_\beta$. The third boundary condition states that there is no flux across the impermeable interface between the α and σ phases, $A_{\alpha\sigma}$.

The volume averaging method seeks to smooth spatial variations due to the complex geometrical structure of a porous medium through a rigorous mathematical process.[37] This procedure is applicable to the present experimental studies since the experimental measurements are made over time scales (diffusion time Δ of order 10 ms) long enough for the probe species, in this case water, to travel several micrometers, and the major heterogeneities of the Pluronic media are on the length scale of 5−20 nm. In other words, the experiments provide diffusion coefficients that are averaged over regions of order 10 μm which contain of order thousands of Pluronic micelles. Application of the volume average, the volume averaging theorem, a number of length scale restrictions, and the single equation approximation are used to determine the effective diffusion coefficient of a small solute in the three-phase system (details are shown in the Appendix). The result for the present problem is

$$\frac{\partial\{C\}}{\partial t} = D_{eff}\vec{\nabla}^2\{C\} \tag{7}$$

where $\{C\}$ is a single equilibrium weighted phase average concentration, and the nondimensional effective diffusion coefficient is given by

$$D^* = \frac{D_{eff}}{D_\beta}[\epsilon_\sigma K_{eq} + \epsilon_\beta] = \frac{2\bar{\kappa}(1-\epsilon_\alpha) - \epsilon_\beta[\bar{\kappa}(2-\epsilon_p^{-1}\epsilon_\sigma) + \epsilon_p^{-1}\epsilon_\sigma - 2] + \alpha_\sigma\epsilon_\beta\epsilon_\sigma\epsilon_p^{-3/2}}{3-\epsilon_p^{-1}\epsilon_\sigma + \epsilon_\alpha(1+\bar{\kappa}) - \bar{\kappa}(1-\epsilon_p^{-1}\epsilon_\sigma) + \epsilon_\beta(\bar{\kappa}-1) + \alpha_\sigma\epsilon_p^{-3/2}\epsilon_\sigma(2-\epsilon_\beta)} \tag{8}$$

where

$$\bar{\kappa} = \frac{D_\sigma K_{eq}}{D_\beta} \qquad \alpha_\sigma = \frac{2D_\sigma}{I_{ch}P}$$

I_{ch} is the characteristic length of the unit cell and $\epsilon_p = \epsilon_\alpha + \epsilon_\beta$. When $\epsilon_\alpha = 0$, this equation reduces to the result of a similar analysis by Ochoa[45] for the case of a two-phase system.

Parameter Estimation

Before the experimental data can be compared to the volume averaging theory, the variables and parameters in eq 8 need to be evaluated for the Pluronic system. Physical and geometrical arguments can be used to determine how the volume fractions vary with the Pluronic concentration, defined as $C_{Pl} = A/W$ where A is grams of Pluronic F127 added to W milliliters of solution. The density of Pluronic is approximately 1 g/mL,[17] giving a total volume as $V = A + W$. Of the A grams of Pluronic, let x grams be PPO, which also has a density of 1 g/mL.[17] This gives an α phase volume fraction of

$$\epsilon_\alpha = \frac{x}{A+W} \tag{9}$$

The x term can be related to A using the molecular weight of Pluronic F127 [$(EO)_{100}(PO)_{70}(EO)_{100}$] (13 388 g/mol)[9] and the molecular weight of a propylene oxide unit in a chain (56 g/mol). These give

$$\frac{x}{A} = \frac{70(56)}{13388} = 0.3 \tag{10}$$

Substituting eq 10 into eq 9 and using $V = A + W$ yields

$$\epsilon_\alpha = \frac{0.3\,A}{A+W} = \frac{0.3C_{Pl}}{C_{Pl}+1} \tag{11}$$

The total number of micelles in the sample can be determined from the volume of one micelle. In one micelle, the volume occupied by the α phase is given by

$$V'_\alpha = \frac{4}{3}\pi {r_b}^3 \tag{12}$$

where r_b is the radius of the $\alpha-\sigma$ interface. Therefore, the total number of micelles in the sample is

$$N = \frac{\epsilon_\alpha(A+W)}{V'_\alpha} = \frac{x}{V'_\alpha} \tag{13}$$

The volume occupied by the σ phase of one micelle is

$$V'_\sigma = \frac{4}{3}\pi((m r_b)^3 - {r_b}^3) = \frac{4}{3}\pi {r_b}^3(m^3-1) \tag{14}$$

where m is defined as r_a/r_b and r_a is the radius of the $\beta-\sigma$ interface. Multiplying by the number of micelles and dividing by the total volume gives the following σ phase volume fraction

$$\epsilon_\sigma = \frac{NV'_\sigma}{A+W} = \frac{V'_\sigma}{V'_\alpha}\epsilon_\alpha = (m^3-1)\epsilon_\alpha \tag{15}$$

Since the volume fractions must sum to one, the β phase volume fraction is

$$\epsilon_\beta = 1 - \epsilon_\alpha - \epsilon_\sigma \tag{16}$$

Expressing all three volume fractions as functions of concentration gives

$$\epsilon_\alpha = \frac{0.3C_{Pl}}{C_{Pl}+1} \tag{17}$$

$$\epsilon_\sigma = \frac{0.3C_{Pl}(m^3-1)}{C_{Pl}+1} \tag{18}$$

$$\epsilon_\beta = 1 - \frac{0.3C_{Pl}m^3}{C_{Pl}+1} \tag{19}$$

It should be noted that the preceding analysis assumes nonoverlapping spheres.

The specific approach for applying eqs 17−19 to the experimental data will depend on whether the Pluronic system is in the solution phase or the liquid crystalline phase. For the solution phase case m can be assumed to be independent of concentration in the Pluronic since the micelles do not change size. However, in the liquid crystalline phase, the micelles must be close-packed. The restriction on close packing requires ϵ_β to be a constant while the size of the micelle will change to maintain this close packing. It is well established that Pluronic F127 micelles pack in a cubic array,[9] but there is some disagreement over whether the cubic geometry is simple cubic, face-centered cubic, or body-centered cubic.[2,14,15] A close-packed simple cubic array gives $\epsilon_\beta = 0.48$, a face-centered cubic array gives $\epsilon_\beta = 0.26$, and a body-centered cubic array gives $\epsilon_\beta = 0.32$.[46,47]

Table 1. Poly-T Diffusion Data Averages

poly-T	D_{eff} in solution (cm^2/s)	error (cm^2/s)	D_{eff} in Pluronic (cm^2/s)	error (cm^2/s)
T1	4.48E−06[a]	5.70E−07	2.25E−06	1.30E−07
T3	2.08E−06	2.90E−07	1.09E−06	1.31E−07
T5	1.78E−06	3.57E−07	8.41E−07	1.17E−07
T10	1.88E−06	1.36E−07	8.25E−07	8.50E−08
T20	8.39E−07	1.48E−07	5.31E−07	9.20E−08
T30	8.09E−07	1.64E−07	6.38E−07	1.06E−07

[a] Read as 4.48×10^{-6}.

Therefore, in the liquid crystalline phase, ϵ_β is constant, and the other two volume fractions can be expressed as

$$\epsilon_\alpha = \frac{0.3C_{Pl}}{C_{Pl}+1} \tag{20}$$

$$\epsilon_\sigma = 1 - \epsilon_\beta - \frac{0.3C_{Pl}}{C_{Pl}+1} \tag{21}$$

Using eq 19, m can be determined as a function of concentration for the gel-like phase

$$m = \left(\frac{(1-\epsilon_\beta)(C_{Pl}+1)}{0.3C_{Pl}}\right)^{1/3} \tag{22}$$

Therefore, once one of the cubic geometries is assumed, the volume fractions and m can be calculated. Rill et al.[4] and Wanka et al.[9] determined m to be 2.0 for 28% Pluronic. The above analysis yields $m = 2.0$ for simple cubic and $m = 2.2$ for face-centered cubic and body-centered cubic, supporting the simple cubic geometry at this concentration.

The volume fraction of water in the σ phase can also be determined from these relationships. Since $x = 0.3A$, the mass of EO in the sample is $y = 0.7A$. Therefore, the volume of EO in the σ phase, assuming that all of the EO is in the σ phase and that EO has a density of 1 g/mL,[17] is $V_{EO}^\sigma = 0.7A$. The σ phase volume fraction can be defined as

$$\epsilon_\sigma = \frac{V_{EO}^\sigma + V_W^\sigma}{V} \tag{23}$$

where V_W^σ is the total volume of water in the σ phase. The volume fraction of water in the σ phase can therefore be determined from

$$\epsilon_W^\sigma = \frac{V_W^\sigma}{V_W^\sigma + V_{EO}^\sigma} = \frac{\epsilon_\sigma(C_{Pl}+1) - 0.7C}{\epsilon_\sigma(C_{Pl}+1)} \tag{24}$$

Results and Discussion

Oligonucleotide Diffusion: Effect of Solute Size. Table 1 gives the average values of the oligonucleotide self-diffusion coefficients in solutions (without Pluronics) and in Pluronics gels with their experimental errors, and these results are plotted in Figure 3. The effective diffusivity in solution ranges from 4.48×10^{-6} cm^2/s for T_1 to 8.09×10^{-7} cm^2/s for T_{30}. The effective diffusivity in Pluronic ranges from 2.25×10^{-6} cm^2/s for T_1 to 5.31×10^{-7} cm^2/s for T_{20} and 6.38×10^{-7} cm^2/s for T_{30}.

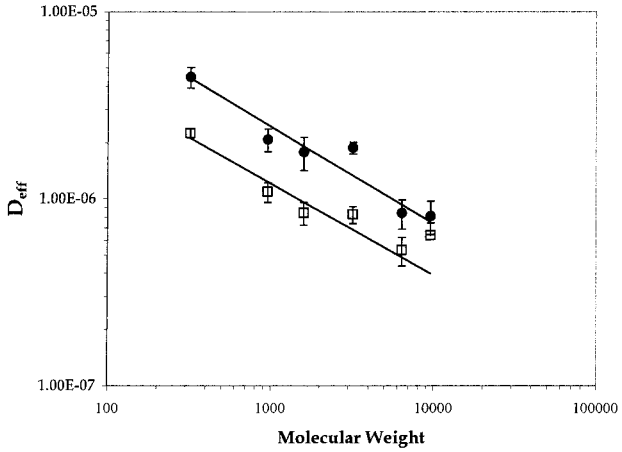

Figure 3. Diffusion coefficients of poly-T's in buffer solution (without Pluronic) (solid circles) and effective diffusion coefficients of poly-T's in 20% Pluronic plotted as functions of molecular weight. For the buffer solution case $R^2 = 0.941$ and for the Pluronic gel case $R^2 = 0.930$.

To compare the data with the diffusion models, the data were fit to a power law function of the form

$$D_{\text{eff}} \propto M^b \tag{25}$$

where M represents the molecular weight of the polymer chain. The solution data were fit directly to eq 25 using a weighted nonlinear least-squares method and gave $b = -0.52 \pm 0.07$ with an R^2 value of 0.941 and a proportionality constant of 8.86×10^{-5} cm^2/s. The regression curve passes through or near all of the error bars except for T_{10}, indicating possible additional experimental error associated with this point. In general, however, the Zimm[25,21] model, which predicts $b = -0.5$, therefore describes fairly well the effect of molecular weight on the diffusion coefficient of the oligonucleotides in solution.

For comparison, Yang et al.[48] found by PFGNMR that the diffusion coefficient of *d*(CGCGTTTTGCGC) in solution was 1.36×10^{-6} cm^2/s. The regression equation for the oligonucleotide data for the present study predicts a diffusion coefficient of 1.25×10^{-6} cm^2/s for a chain of 12 oligonucleotides. The difference of only 8% from the experiments of Yang et al.[48] may be attributed to the different nucleotides and experimental errors.

The results for the oligonucleotide diffusion measurements in Pluronic are also shown in Figure 3. The data for diffusion in Pluronic were also fit directly to eq 25 and gave $b = -0.49 \pm 0.07$ with an R^2 value of 0.930 and proportionality constant of 3.57×10^{-5} cm^2/s. In this case the regression curve passes through or near all of the error bars except for T_{30}. However, in general, the result implies that diffusion of oligonucleotides in Pluronic gel-like phases also follow Zimm theory.[25]

Using the Kratky−Porod[49,21] model for wormlike coils, a chain length of 0.7 nm per nucleotide, and a persistence length of 5 nm the mean end-to-end distance of T_{10}, T_{20}, and T_{30} is 5.7, 9.7, and 12.7 nm, respectively. In comparison, a porous medium with simple cubic geometry of close-packed spherical particles with 18 nm center-to-center spacing would have cavities (larger spaces between particles) of 6.5 nm radius separated by narrower constrictions of 3.7 nm radius. Other packing unit geometry would lead to slightly smaller constrictions and pore openings. The present diffusion data therefore indicate that the narrow constrictions are not severe enough to highly restrict the diffusion of the oligonucleotides in this size range. These results are reasonable and point to the need for further experiments with longer oligonucleotides.

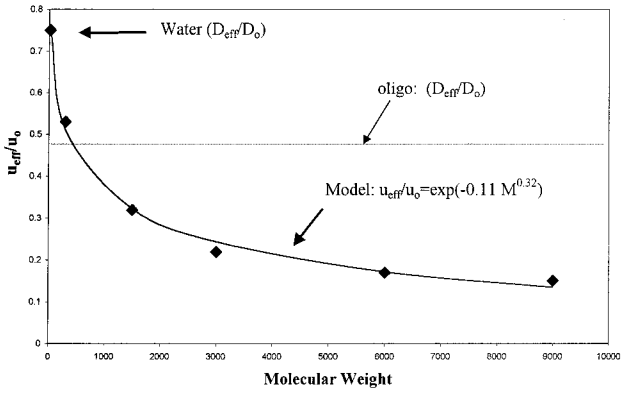

Figure 4. Electrophoretic mobility ratios of poly-T's from the literature[20,50] as a function of molecular weight.

The ratio of the effective diffusivities of the oligonucleotides in the Pluronic gel to the diffusivities in the buffer solution without Pluronics is approximately 0.5. Although there is some minor variability in this result at the highest molecular weight due to the seemingly large diffusion coefficient of the T-30 in the Pluronic gel, it is clear from Figure 3 that the ratio of the diffusion coefficients is approximately independent of the molecular size. This indicates that the effects of the Pluronic on restricting diffusion is not related to the size of the molecules.

Previous results have shown that the electrophoretic mobility of oligonucleotides (T_{12}−T_{18}) varies with molecular weight as $M^{-0.36}$ in a 20% Pluronic gel.[20] The free solution mobility can be obtained through extrapolation to zero gel concentration of measured mobility for a series of different concentration Pluronic. This result implies a single free solution mobility of about 4.4×10^{-4} cm^2/(V s) for molecules in this range.[20] This result is very close to the measured value of 4.0×10^{-4} cm^2/(V s) for T_{10} to T_{60}.[50] Grossman,[50] through measurements with capillary electrophoresis, also found that the mobility of T_3 was 2.5×10^{-4} cm^2/(V s), that of T_5 was 3.5×10^{-4} cm^2/(V s), that of T_{10} was 4.0×10^{-4} cm^2/(V s), and above T_{10} the mobility no longer depended upon molecular size. These results, which show increasing mobility with molecular size until a limiting value is obtained, are consistent with experimental results of small DNA[51,52] and theoretical predictions from molecular dynamics and other approaches.[53,54]

The ratio of the electrophoretic mobilities in the gel to those in free solution can be determined using the free solution electrophoretic mobilities and the measured mobilities in 20% Pluronic from the literature. These ratios varied from 0.53 for T_3, 0.32 for T_5, 0.22 for T_{10}, 0.17 for T_{20}, and 0.15 for T_{30}. (Note that the values for the mobilities in the Pluronic for these estimates were extrapolated from the scaling law obtained with the measurements of T_{12} to T_{18}.) Figure 4 shows the electrophoretic mobility plotted verses the molecular weight for the T-oligomers, and included for reference is a line for the constant diffusion coefficient ratio (=0.5). The value of the mobility ratio for T_3 is quite close to the diffusion coefficient ratio, and this is consistent with the standard Ogston[55]−Morris[56]−Rodbard[57]−Chrambach[19] (OMRC) electrophoresis theory. The conjecture that the mobility ratio equals the diffu-

sion coefficient ratio was first postulated by Morris,[56] and more recent theoretical analysis has shown this to be valid only for small solutes in nonpercolating media with small concentration of obstacles.[58,59] The OMRC model also predicts that the mobility ratio (equal to the diffusion coefficient ratio) will equal the volume fraction of space available to the given solute, and this also appears to be valid for the T_3 (see also discussion below for water self-diffusion results). However, as the oligonucleotide size increases, the mobility ratio decreases to 0.15 for the T_{30}, and this value is over 3 times less than the diffusion coefficient ratio. Clearly the diffusion ratio part of the OMRC model is not valid for the larger size molecules.

It is interesting to note that the stretched exponential function, given in eq 26

$$\frac{D_{\text{eff}}}{D_0} = \frac{u_{\text{eff}}}{u_0} = \exp(-aM^b) \tag{26}$$

commonly used to describe diffusion,[62−66] and electrophoresis,[67,68] of globular macromolecules in porous media does not describe the diffusion data since there is no molecular weight dependence of the diffusion coefficient ratio. However, this equation (as shown in Figure 4) describes the electrophoresis data. In contrast, Gibbs and Johnson[43] found that eq 26 was followed for both diffusion and electrophoresis of moderate molecular weight species in polyacrylamide gels, and assuming that the hydrodynamic radius $R_H = M^{1/3}$, their data implies $b = 0.17$. Equation 26 is consistent with the OMRC model when the coefficient $b = 0.67$. Since the electrophoretic mobilities of the oligonucleotides in Pluronic, as shown in Figure 4, give $b = 0.32$, the OMRC model also does not describe the size dependence of the electrophoretic mobility in Pluronic, and the size dependence of the mobility in Pluronic is different from that in polyacrylamide.

Baumgartner and Muthukumar[23,60] and Melenkevitz and Muthukumar[61] have performed Monte Carlo simulations of diffusion and electrophoresis of polyelectrolytes in a number of model porous media structures. They identified three regimes for diffusive and electrophoretic behavior: (I) for molecules with chain size much smaller than the average pore size motion is equivalent to that of point particles and restrictions are due to geometrical constraints of the media, (II) for molecules with chain size comparable to the average pore size the so-called entropic barrier governs transport through the constrictions, and (III) when the chain size is much larger than the average pore size reptation-like behavior governs. Most of the oligonucleotide experiments in the present study fall in regime I; however, the largest molecule, T_{30}, has a radius of gyration of 1.6 nm, which is about $^1/_2$ of the size of the largest constriction for simple cubic geometry as mentioned above. One may therefore consider this size solute to fall in the transition between regime I and II. Muthukumar and Baumgarter[60] find that the diffusion coefficient ratio decreases exponentially with polymer length for regime II when the size of the constrictions between obstacles is large, but when the constrictions are small the diffusion ratio is independent of the molecular size and only depends on the size of the constrictions. For regime III Melenkevitz and Muthukumar[61] find by MC simulations in random three-dimensional media of cubic obstacles that the electrophoretic mobility scales as $M^{-0.27}$. Furthermore, their simulations for diffusion in free solution imply Rouse behavior, scaling with M^{-1}, which is also not observed in the present experiments.

Table 2. Water Diffusion Coefficients (10^{-5} cm^2/s) as a Function of Pluronic Concentration

Pluronic conc (%)	diff coeff	SD of mean	Pluronic conc (%)	diff coeff	SD of mean
0	2.19	0.02	20	1.64	0.04
10	1.78	0.03	25	1.43	0.04
15	1.76	0.05	30	1.41	0.05

The present results therefore indicate that, with respect to diffusive transport in Pluronic, oligonucleotides behave as in free solution giving rise to no molecular size dependence of the diffusion coefficient ratio. However, with respect to electrophoretic transport, oligonucleotides have a larger size dependence ($b = 0.32$ in eq 26) than similar size molecules in conventional polyacrylamide gels ($b = 0.17$). Although further work is necessary to investigate this phenomenon, it appears that when no electrical field is driving the molecules through the Pluronic, diffusion is relatively unconstrained by the presence of the micelles, at least with respect to molecular size dependent factors. In the presence of an electrical field the oligonucleotides may have size-dependent interactions with the hydrophilic PEO domains of the Pluronic micelles. These interactions may result from local variations of the electrical field as it propagates through and around the micelle. Since PEO is hydrophilic, the electrical field may propagate through this domain while propagating around the hydrophobic PPO domain. If the electrical field serves to pull the oligonucleotides through the PEO domain, a size-dependent mobility may result.

Water Diffusion: Effects of Media Geometry. The water self-diffusion coefficients obtained in the present study (given in Table 2), in addition to the diffusion measurements made by Malmsten and Lindman,[17] are compared to the volume averaging theory. Malmsten and Lindman[17] measured water diffusion in aqueous systems of Pluronic F127 by NMR as the concentration was varied from 1% to 67%. In their system, the transition between the solution phase and the liquid crystalline phase occurred at 28%, which is somewhat different from the 20% for the present experiments, and this discrepancy may be attributed to the presence of cosolutes in the current study.

Since the behavior of the system with respect to available volume fractions is expected to differ from solution phase to gel-like phase, it is reasonable to fit the data for these two regions separately. Consider first the data for the liquid crystalline phase. Since this is a gel-like phase, ϵ_β is set to a constant value for one of the three specified cubic geometries, and ϵ_α and ϵ_σ are calculated according to eqs 20 and 21. Neglecting mass transfer effects requires $\alpha_\sigma = 0$, and the adjustable parameters left in eq 8 are K_{eq} and D_σ. Equation 8 with K_{eq} and D_σ as adjustable parameters could not be fit to the data from the current study and from Malmsten and Lindman.[17] This is due to the fact that the small variations of ϵ_σ and ϵ_α that result from variation of Pluronic concentration cannot describe the larger variations in D_{eff} that are observed when K_{eq} and D_σ are held constant. Increases in Pluronic concentration imply a decrease in the volume fraction of water in the σ phase, which the theory cannot account for when K_{eq} and D_σ are held constant. Since D_σ is expected to decrease with

Table 3. D_σ Values as a Function of Concentration for the Liquid Crystalline Phase ($K_{eq} = 1$)

	$\epsilon_\beta = 0.48$			$\epsilon_\beta = 0.32$			$\epsilon_\beta = 0.26$		
concn (%)	ϵ_σ	ϵ_w^σ	D_σ/D_β	ϵ_σ	ϵ_w^σ	D_σ/D_β	ϵ_σ	ϵ_w^σ	D_σ/D_β
Data from Malmsten and Lindman (1992b)									
33	0.446	0.611	0.479	0.606	0.713	0.586	0.666	0.739	0.615
43	0.430	0.510	0.378	0.590	0.643	0.504	0.650	0.676	0.538
54	0.415	0.409	0.340	0.575	0.573	0.476	0.635	0.613	0.513
67	0.400	0.298	0.180	0.560	0.499	0.346	0.620	0.547	0.391
Data from Present Study									
20	0.470	0.752	0.621	0.630	0.815	0.700	0.690	0.831	0.722
25	0.460	0.696	0.461	0.620	0.774	0.568	0.680	0.794	0.598
30	0.451	0.642	0.451	0.611	0.736	0.561	0.671	0.759	0.591

decreasing ϵ_W^σ, setting D_σ to a constant value is therefore not reasonable, and it will be considered to vary as discussed below.

D_σ is an effective diffusion coefficient that represents the restrictions to water transport within the network of polymer chains in the PEO region of the Pluronic. It is therefore useful to consider some of the many models that describe diffusion in porous media as a function of porosity. For example, Maxwell's[69] equation, given by

$$\frac{D_\sigma}{D_0} = \frac{2\epsilon_\sigma}{3 - \epsilon_\sigma} \tag{27}$$

is an upper bound for the relative diffusion coefficients in isotropic media. Archie[70] obtained an empirical relationship

$$\frac{D_\sigma}{D_0} = \epsilon_\sigma^z \tag{28}$$

where z is determined experimentally. Perrins et al.[71] derived the following expression for cylindrical fibers in a square lattice

$$\frac{D_\sigma}{D_0} = 1 - \frac{2\phi}{1 + \phi - \dfrac{0.305827\phi^4}{1 - 1.402958\phi^8} - 0.013362\phi^8} \tag{29}$$

where $\phi = 1 - \epsilon_\sigma$. Volume averaging[37,45,72,73] has also been used for such systems, and it has been shown that the numerical results for an isotropic two-phase system using volume averaging are quite close to the results from eq 29. Wakao and Smith[74] found the expression

$$\frac{D_\sigma}{D_0} = \epsilon_\sigma^2 \tag{30}$$

Last, Mackie and Meares[30] obtained the equation

$$\frac{D_\sigma}{D_0} = \left(\frac{\epsilon_\sigma}{2 - \epsilon_\sigma}\right)^2 \tag{31}$$

This latter equation is often used to describe diffusion in polymers when the polymer fibers are of the same order of magnitude as the solute.

The experimental data for the water diffusion coefficients in the Pluronic of variable concentrations were fit to eq 8 using $K_{eq} = 1$, $\alpha = 0$ to determine the one unknown parameter D_σ, and these results are given in Table 3. Note that the value of the volume fraction ϵ_β is based upon the three possible unit cell geometries under consideration and that the other two volume fractions

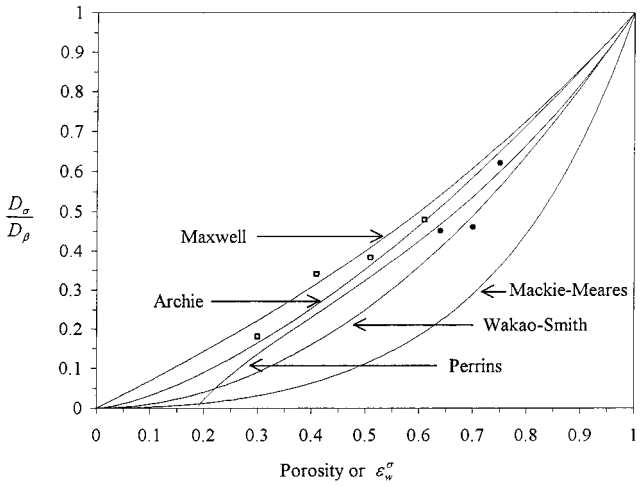

Figure 5. Effective water diffusion coefficients in the σ phase plotted as a function of porosity for simple cubic packing ($\epsilon_\beta = 0.48$). Comparison with various diffusion models. The circles are data from the present study, and the squares are data from Malmsten and Lindman.[17]

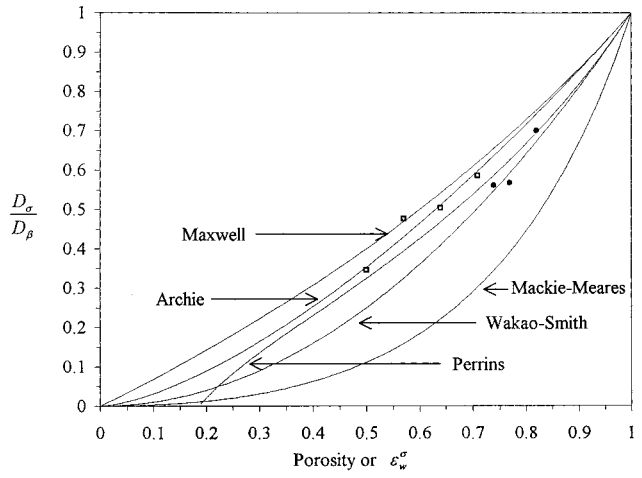

Figure 6. Effective water diffusion coefficients in the σ phase plotted as a function of porosity for body-centered-cubic packing ($\epsilon_\beta = 0.32$). Comparison with various diffusion models. The circles are data from the present study, and the squares are data from Malmsten and Lindman.[17]

are calculated from the gel composition. The resulting diffusion coefficients, D_σ, are shown in Figures 5−7 as functions of porosity and compared with the above diffusion models. Figure 5 shows the results for simple cubic geometry, Figure 6 shows the results for body-centered-cubic geometry, and Figure 7 shows the results for face-centered-cubic geometry. In general, the Perrins et al.[71] model and the Archie[70] model with $z = 1.5$ fit the Malmsten and Lindman[17] data reasonably well, although there is some scatter about these curves. The

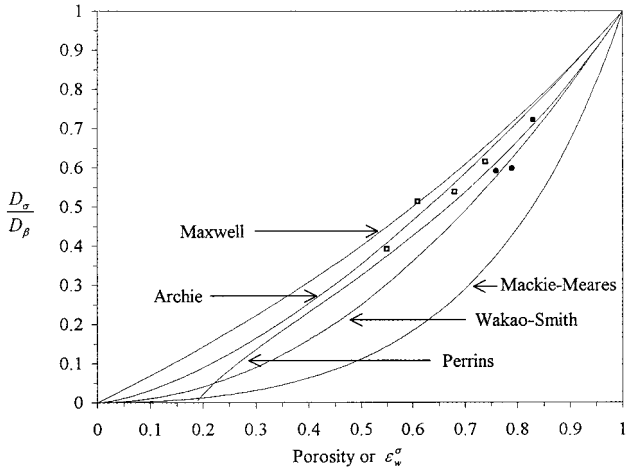

Figure 7. Effective water diffusion coefficients in the σ phase plotted as a function of porosity for face-centered-cubic packing ($\epsilon_\beta = 0.26$). Comparison with various diffusion models. The circles are data from the present study, and the squares are data from Malmsten and Lindman.[17]

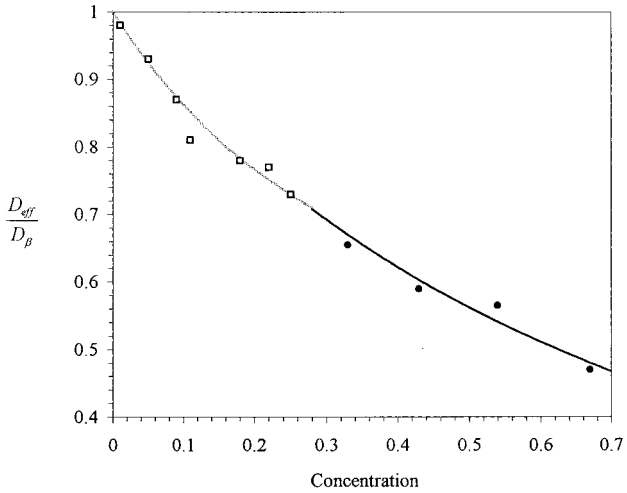

Figure 8. Water diffusion data from Mamsten and Lindman[17] plotted as a function of Pluronic concentration. The squares represent the solution phase, while the circles represent the liquid crystalline phase. The two curves represent the volume averaging theory for the different regions.

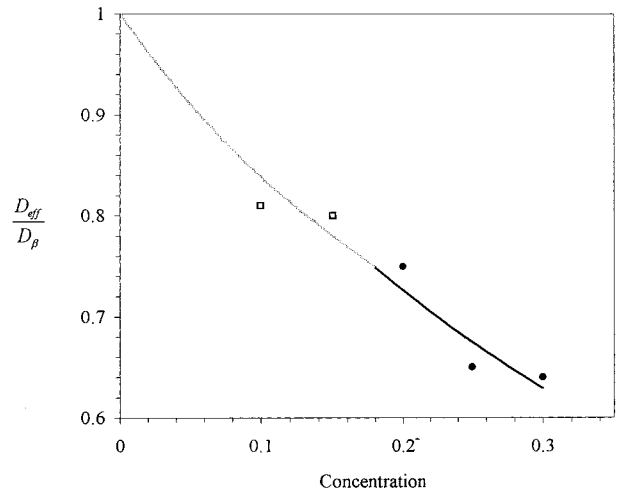

Figure 9. Water diffusion data from current study plotted as a function of Pluronic concentration. The squares represent the solution phase, while the circles represent the liquid crystalline phase. The two curves represent the volume averaging theory for the different regions.

Perrins et al.[71] model and the Archie[70] model with $z = 2.0$ fit the data from the current study reasonably well. In both cases, there is some degree of scatter; however, the overall fit of the models to the data is fairly good considering there are no adjustable parameters, at least in the Perrins model, in this part of the analysis. Furthermore, this result is encouraging since the Perrins et al.[71] model was derived for cylindrical fibers that may resemble the EO chains. In general, the fits to the experimental data show that the Mackie−Meares model is the farthest from the data and that the data are clustered around the other theories. Experiments over a wider range of volume fractions are needed in order to more fully test and discriminate among these various theories.

In the solution phase, m can be assumed independent of Pluronic concentration, and the volume fractions can be calculated according to eqs 17−19, with m as an adjustable parameter. Since the experimental data show no observable discontinuity in the diffusion behavior as the concentration of Pluronic varies from the solution phase to the gel-like phase, eq 8 was fit to the data in the solution phase with the constraint that there is a smooth transition from the gel-like phase to the solution phase. The resulting fits for the data from Malmsten and Lindman[17] are shown in Figure 8. For the liquid crystalline phase, $\epsilon_\beta = 0.26$, $K_{eq} = 1$, and the z from the Archie model is 1.5. For the solution phase, $D_\sigma/D_\beta = 0.68$, $K_{eq} = 1.5$, and $m = 2.2$. Assuming the radius of the $\alpha-\sigma$ interface, r_b, is 4.5 nm,[4,9] an m of 2.2 gives a radius of 10 nm for the entire micelle. Wanka et al.[9] report a radius of 10.1 nm for 14% solutions of Pluronic, which is in the solution phase, lending credibility to the current analysis.

The results for an analysis similar to the one described above applied to the water self-diffusion data of the current study are shown in Figure 9. For the liquid crystalline phase, $\epsilon_\beta = 0.26$, $K_{eq} = 1$, and the z from the Archie[70] model is 2.0. For the solution phase, $D_\sigma/D_\beta = 0.66$, $K_{eq} = 1.5$, and $m = 2.3$.

Pluronic in the solution phase was assumed to consist of micelles whose size is essentially independent of concentration. As the concentration increases, the volume fractions of the three phases change because of an increase in the number of micelles per unit volume. Physical parameters such as D_σ and K_{eq} were assumed independent of concentration in this region. Pluronic in the liquid crystalline phase was assumed to be close-packed nonoverlapping micelles whose size is a function of concentration. Since the spheres are close-packed and nonoverlapping, ϵ_β is constant. As the concentration changes, the volume fractions of the α and σ phases change, but not significantly. The major response of the liquid crystalline system to a change in concentration is a change in composition of the σ phase. As the concentration increases, the volume fraction of water in the σ phase decreases. Therefore, D_σ is a function of Pluronic concentration in the gel-like region and can be described by diffusion models such as the Perrins and Archie equations for two-phase porous media. Using the above models, the volume averaging theory is thus able to describe the water self-diffusion data in a continuous fashion.

The assumption of nonoverlapping spherical micelles in the liquid phase of the Pluronics facilitates the development of the closed form solution for the effective diffusion coefficient (eq 8) using the method of volume

averaging. In principle, this method can be applied to any specified unit cell of a given geometry; however, numerical calculations would be required to evaluate the results. A detailed evaluation of these effects will be left for future work; however, some qualitative considerations can be made on the basis of the present results. In general, the consequences of accounting for overlap of the σ phase would lead to a reduction in the volume fraction of the β phase and therefore an increase in the volume fraction of the σ phase. The larger σ phase would imply that the volume fraction of water in the σ phase would therefore be larger than that found presently, thus giving rise to a larger effective diffusion coefficient in the σ phase. The increased contributions of the effective diffusion in the σ phase to the overall observed effective diffusion would compensate the reduced contributions of the diffusion in the β phase and may not significantly change the general trends of the overall fit to the experimental results. Detailed evaluation of the relative contributions of water diffusion in the β phase and the σ phase requires experimental measurements of water diffusion in systems of poly(ethylene oxide) as a function of the concentration of the poly(ethylene oxide).

The ratio of the effective diffusion coefficients of the oligonucleotides in Pluronic to those in free solution was found to be 0.5. Since this result indicates no size dependence of the diffusion ratio of oligonucleotides in the Pluronic, application of eq 8 would be useful to determine the restrictions due to media geometry. Assuming the oligonucleotides cannot enter the σ phase, $K_{eq} = \bar{\kappa} = 0$. In addition, for $\epsilon_\beta = 0.26$, eqs 20 and 21 give $\epsilon_\alpha = 0.05$ and $\epsilon_\sigma = 0.69$ for 20% solutions of Pluronic F127. These values lead to $D^* = 0.15$ from eq 8 and

$$\frac{D_{eff}}{D_\beta} = 0.58 \tag{32}$$

Equation 32 implies that the maximum reduction in the diffusion coefficient for point solutes that do not enter the σ phase is 42%. For the oligonucleotides, the reduction was 49%. Therefore, the reduction in diffusion coefficients for oligonucleotides by the Pluronic can be accounted for primarily by geometrical restrictions of the system. The additional 7% reduction may be due to chemical and physical interactions between the oligonucleotides and the Pluronic micelles (PEO region) or experimental error. This estimate is based upon the assumption that all sizes of the oligonucleotides do not partition into the σ phase, i.e., $K_{eq} = 0$; however, if the small oligomers could partition into the σ phase of the Pluronic, the restriction on the diffusion coefficient would depend on the value of D_σ for the oligomers. Increasing K_{eq}, holding D_σ fixed, will increase the overall effective diffusion coefficient reflecting an increase in the space available for diffusion. However, increasing K_{eq}, holding κ fixed or decreased, will decrease the effective diffusion coefficient. This increase of K_{eq}, holding κ fixed or decreasing it, implies a decrease in D_σ (through the definition of κ), thereby reflecting less freedom for transport of oligomer within the σ phase. Experimental measurements of oligomer diffusion and electrophoresis within solutions of PEO as well as information addressing the partition coefficient for oligomers into the PEO domain of the Pluronic are necessary to fully address these remaining issues.

Conclusions

Oligonucleotide and water self-diffusion coefficients were measured within the Pluronic copolymer liquid crystal system. The method of volume averaging was used to determine a function to describe the effective diffusion coefficients of solutes in terms of the volume fractions of the three different phases that comprise the media. Parameters in the equation include $\bar{\kappa}$, which depends on the equilibrium distribution coefficient and the diffusion coefficients for the β and σ phases, and α_σ, which reflects resistance to interfacial mass transfer.

Effective water self-diffusion coefficients were measured as a function of the concentration of Pluronic. These data were compared to the volume averaging theory, allowing for estimation of one parameter in eq 8, namely the diffusion coefficient in the σ phase. This diffusion coefficient, D_σ, in turn compared favorably with several theoretical expressions from the literature with respect to its dependence upon volume fraction in the σ phase. These results provide a good indication that the volume averaging theory is a valid descriptive tool for the diffusion of small solutes in Pluronic copolymer liquid crystal system.

Diffusion of the oligonucleotides in solution (without Pluronic) followed the Zimm model for dilute polymer solutions. Diffusion of the oligonucleotides in the Pluronic system also followed the Zimm model, demonstrating that polymers in this size range in the Pluronic system still behave as if in dilute solutions. The ratio of the effective diffusion coefficients of the oligonucleotides in the Pluronic to those in solution was determined to be 0.5. This result is remarkable because it indicates no size dependence on diffusion. Using the volume averaging theory, it was determined that the maximum reduction of the diffusion coefficient for point solutes due to geometry alone was 42%. The small 7% further reduction for the oligonucleotides can be attributed to some combination of physical and chemical interactions between the oligonucleotides and the Pluronic micelles and, perhaps, experimental error. These results, when compared to electrophoretic mobility measurements of oligonucleotides in Pluronic gels, indicate that while olignonucleotide diffusion in Pluronic relative to diffusion in free solution is independent of molecular size and is reduced primarily by geometrical constraints, electrophoresis in Pluronic relative to free solution electrophoresis is reduced by size-dependent factors. The latter may be a result of the specific physical-chemical nature of the PEO−PPO−PEO micelle structure consisting of a hydrophobic electrically insulating core surrounded by hydrophilic electrically conducting domains.

Acknowledgment. We gratefully acknowledge NASA (Grant NAG81163) for support of this work. Discussions with Dr. Timothy Moerland and Dr. Stephen Gibbs were very helpful in the conduction of the experimental portion of this work. We also thank Mr. Richard Rosanske and Dr. Thomas Gedris for help in building the NMR probe and Mr. Hank Hendricks and Dr. Umesh Goli of the Biochemical Analysis and Synthesis Service (BASS) Lab at Florida State University for preparing the oligonucleotides.

Appendix

The following derivation closely follows the methods developed by Ryan et al.,[72] Nozad et al.,[75] and Ochoa.[45]

In addition to the boundary conditions given in the text, it is necessary to impose the following boundary conditions on the entrances and exits of the averaging volume

$$\text{BC 4a:} \quad C_\beta = F(\vec{r},t) \quad \text{at } A_{\beta e} \tag{A1}$$

$$\text{BC 4b:} \quad C_\sigma = G(\vec{r},t) \quad \text{at } A_{\sigma e} \tag{A2}$$

$$\text{BC 4c:} \quad C_\alpha = 0 \quad \text{at } A_{\alpha e} \tag{A3}$$

Boundary conditions 4a and 4b define C_β and C_σ as functions of space and time at the entrances and exits to the β and σ phases, $A_{\beta e}$ and $A_{\sigma e}$, respectively. Boundary condition 4c states that C_α is zero since the α phase is impermeable to the solute. The major difference between this development and previous work[45] is the addition of the impermeable α phase, which necessitates boundary conditions 3 (in text) and 4c above.

With every point in space there is an associated averaging volume V. Applying the volume average to eq A2 gives

$$\frac{1}{V}\int_{V_\sigma} \frac{\partial C_\sigma}{\partial t}\, dV = \frac{1}{V}\int_{V_\sigma} \vec{\nabla}\cdot(D_\sigma \vec{\nabla} C_\sigma)\, dV \tag{A4}$$

Carbonell and Whitaker[76] derive the constraints on the length scales involved in volume averaging in detail. For the present system, the constraints are

$$l_\alpha,\ l_\beta,\ l_\sigma \ll r_0 \ll L \tag{A5}$$

where the left-hand terms are the characteristic lengths of the α, β, and σ phases, respectively, r_0 is the characteristic radius of the averaging volume, and L is the characteristic length of the macroscopic system. In the current study, l_α, l_β, and l_σ are on the order of 1−20 nm, L is on the order of 1 cm, and r_0 represents the length scale associated with the diffusion time of the NMR experiments, which is approximately 7 μm. The phase average concentration is given by

$$\langle C_\sigma \rangle = \frac{1}{V}\int_{V_\sigma} C_\sigma\, dV \tag{A6}$$

Restricting the analysis to rigid porous media, eq A4 can be written as

$$\frac{\partial \langle C_\sigma \rangle}{\partial t} = \langle \vec{\nabla}\cdot(D_\sigma \vec{\nabla} C_\sigma) \rangle \tag{A7}$$

Application of the volume averaging theorem[44,77,78] gives

$$\frac{\partial \langle C_\sigma \rangle}{\partial t} = \vec{\nabla}\cdot\langle D_\sigma \vec{\nabla} C_\sigma \rangle + \frac{1}{V}\int_{A_{\beta\sigma}} \hat{n}_{\sigma\beta}\cdot D_\sigma \vec{\nabla} C_\sigma\, dA + \frac{1}{V}\int_{A_{\alpha\sigma}} \hat{n}_{\sigma\alpha}\cdot D_\sigma \vec{\nabla} C_\sigma\, dA \tag{A8}$$

Using the third boundary condition, the last term of eq A8 is zero. A second application of the volume averaging theorem yields

$$\frac{\partial \langle C_\sigma \rangle}{\partial t} = \vec{\nabla}\cdot\left\{ D_\sigma \left[\vec{\nabla}\langle C_\sigma \rangle + \frac{1}{V}\int_{A_{\alpha\sigma}} \hat{n}_{\sigma\beta} C_\sigma\, dA + \frac{1}{V}\int_{A_{\beta\sigma}} \hat{n}_{\sigma\alpha} C_\sigma\, dA \right] \right\} + \frac{1}{V}\int_{A_{\beta\sigma}} \hat{n}_{\sigma\beta}\cdot D_\sigma \vec{\nabla} C_\sigma\, dA \tag{A9}$$

It is usually more convenient to use the intrinsic phase average concentration which is defined as

$$\langle C_\sigma \rangle^\sigma = \frac{1}{V_\sigma}\int_{V_\sigma} C_\sigma\, dV \tag{A10}$$

The intrinsic phase average concentration is related to the phase average concentration by ϵ_σ, which is the volume fraction of the σ phase, by the following relationship

$$\langle C_\sigma \rangle = \epsilon_\sigma \langle C_\sigma \rangle^\sigma \tag{A11}$$

Substitution of eq A11 into eq A9 yields

$$\epsilon_\sigma \frac{\partial \langle C_\sigma \rangle^\sigma}{\partial t} = \vec{\nabla}\cdot\left\{ D_\sigma \left[\vec{\nabla}(\epsilon_\sigma \langle C_\sigma \rangle^\sigma) + \frac{1}{V}\int_{A_{\beta\sigma}} \hat{n}_{\sigma\beta} C_\sigma\, dA + \frac{1}{V}\int_{A_{\alpha\sigma}} \hat{n}_{\sigma\alpha} C_\sigma\, dA \right] \right\} + \frac{1}{V}\int_{A_{\beta\sigma}} \hat{n}_{\sigma\beta}\cdot D_\sigma \vec{\nabla} C_\sigma\, dA \tag{A12}$$

It is now necessary to apply Gray's decomposition[79] in order to define the local spatial deviation concentration as

$$\tilde{C}_\sigma = C_\sigma - \langle C_\sigma \rangle^\sigma \tag{A13}$$

Equation A13 can be used in eq A10 to get

$$\vec{\nabla}(\epsilon_\sigma \langle C_\sigma \rangle^\sigma) + \frac{1}{V}\int_{A_{\beta\sigma}} \hat{n}_{\sigma\beta} C_\sigma\, dA + \frac{1}{V}\int_{A_{\alpha\sigma}} \hat{n}_{\sigma\alpha} C_\sigma\, dA = \epsilon_\sigma \vec{\nabla}\langle C_\sigma \rangle^\sigma + \langle C_\sigma \rangle^\sigma \vec{\nabla}\epsilon_\sigma + \frac{1}{V}\int_{A_{\beta\sigma}} \hat{n}_{\sigma\beta}\langle C_\sigma \rangle^\sigma\, dA + \frac{1}{V}\int_{A_{\beta\sigma}} \hat{n}_{\sigma\beta}\tilde{C}_\sigma\, dA + \frac{1}{V}\int_{A_{\alpha\sigma}} \hat{n}_{\sigma\alpha}\langle C_\sigma \rangle^\sigma\, dA + \frac{1}{V}\int_{A_{\alpha\sigma}} \hat{n}_{\sigma\alpha}\tilde{C}_\sigma\, dA \tag{A14}$$

Carbonell and Whitaker[76] have shown that if the previously defined length constraints are satisfied, the following approximations are valid

$$\frac{1}{V}\int_{A_{\beta\sigma}} \hat{n}_{\sigma\beta}\langle C_\sigma \rangle^\sigma\, dA = \left\{ \frac{1}{V}\int_{A_{\beta\sigma}} \hat{n}_{\sigma\beta}\, dA \right\} \langle C_\sigma \rangle^\sigma \tag{A15}$$

$$\frac{1}{V}\int_{A_{\alpha\sigma}} \hat{n}_{\sigma\alpha}\langle C_\sigma \rangle^\sigma\, dA = \left\{ \frac{1}{V}\int_{A_{\alpha\sigma}} \hat{n}_{\sigma\alpha}\, dA \right\} \langle C_\sigma \rangle^\sigma \tag{A16}$$

It can be shown from the averaging theorem that

$$\frac{1}{V}\int_{A_{\beta\sigma}} \hat{n}_{\sigma\beta}\, dA + \frac{1}{V}\int_{A_{\alpha\sigma}} \hat{n}_{\sigma\alpha}\, dA = -\vec{\nabla}\epsilon_\sigma \tag{A17}$$

Substitution of eqs A15−A17 into eq A14 yields

$$\vec{\nabla}(\epsilon_\sigma \langle C_\sigma \rangle^\sigma) + \frac{1}{V}\int_{A_{\beta\sigma}} \hat{n}_{\sigma\beta} C_\sigma\, dA + \frac{1}{V}\int_{A_{\alpha\sigma}} \hat{n}_{\sigma\alpha} C_\sigma\, dA = \epsilon_\sigma \left[\vec{\nabla}\langle C_\sigma \rangle^\sigma + \frac{1}{V_\sigma}\int_{A_{\beta\sigma}} \hat{n}_{\sigma\beta}\tilde{C}_\sigma\, dA + \frac{1}{V_\sigma}\int_{A_{\alpha\sigma}} \hat{n}_{\sigma\alpha}\tilde{C}_\sigma\, dA \right] \tag{A18}$$

Substitution of eq A18 into eq A12 yields

$$\epsilon_\sigma \frac{\partial \langle C_\sigma \rangle^\sigma}{\partial t} = \vec{\nabla}\cdot\left\{\epsilon_\sigma D_\sigma\left[\vec{\nabla}\langle C_\sigma\rangle^\sigma + \frac{1}{V_\sigma}\int_{A_{\beta\sigma}} \hat{n}_{\sigma\beta}\tilde{C}_\sigma \, dA + \frac{1}{V_\sigma}\int_{A_{\alpha\sigma}} \hat{n}_{\sigma\alpha}\tilde{C}_\sigma \, dA\right]\right\} + \frac{1}{V}\int_{A_{\beta\sigma}} \hat{n}_{\sigma\beta}\cdot D_\sigma \vec{\nabla} C_\sigma \, dA \quad \text{(A19)}$$

An analogous equation for the β phase can be determined. The next step in the volume averaging approach is to invoke the principle of local mass equilibrium[80] to derive a one equation model. It is assumed that the diffusion process can be characterized by a single equilibrium weighted concentration defined as

$$\{C\} = \frac{\epsilon_\sigma}{K_{eq}}\langle C_\sigma\rangle^\sigma + \epsilon_\beta \langle C_\beta\rangle^\beta \quad \text{(A20)}$$

Macroscopic spatial deviation concentrations are defined as

$$\hat{C}_\sigma = \langle C_\sigma\rangle^\sigma - K_{eq}\{C\}, \quad \hat{C}_\beta = \langle C_\beta\rangle^\beta - \{C\} \quad \text{(A21)}$$

When eqs A19−A21 are substituted into eq A19 and the equivalent for the β phase, and the two resulting equations are added, the following equation is obtained

$$(\epsilon_\sigma K_{eq} + \epsilon_\beta)\frac{\partial\{C\}}{\partial t} = \vec{\nabla}\cdot\left\{\epsilon_\beta D_\beta\left[\vec{\nabla}\{C\} + \frac{1}{V_\beta}\int_{A_{\beta\sigma}} \hat{n}_{\beta\sigma}\tilde{C}_\beta \, dA\right] + \epsilon_\sigma D_\sigma\left[K_{eq}\vec{\nabla}\{C\} + \frac{1}{V_\sigma}\int_{A_{\beta\sigma}} \hat{n}_{\sigma\beta}\tilde{C}_\sigma \, dA + \frac{1}{V_\sigma}\int_{A_{\alpha\sigma}} \hat{n}_{\sigma\alpha}\tilde{C}_\sigma \, dA\right]\right\} - \left\{\epsilon_\sigma\frac{\partial\hat{C}_\sigma}{\partial t} + \epsilon_\beta\frac{\partial\hat{C}_\beta}{\partial t} - \vec{\nabla}\cdot(\epsilon_\sigma D_\sigma\vec{\nabla}\hat{C}_\sigma) - \vec{\nabla}\cdot(\epsilon_\beta D_\beta\vec{\nabla}\hat{C}_\beta)\right\} \quad \text{(A22)}$$

The last term of this equation can be neglected when the following inequalities (and equivalents for the β phase) are satisfied

$$\epsilon_\sigma\frac{\partial\hat{C}_\sigma}{\partial t} \ll (\epsilon_\sigma K_{eq} + \epsilon_\beta)\frac{\partial\{C\}}{\partial t} \quad \text{(A23)}$$

$$\hat{C}_\sigma \ll K_{eq}\{C\} \quad \text{(A24)}$$

$$\epsilon_\sigma D_\sigma\vec{\nabla}^2\hat{C}_\sigma \ll (\epsilon_\sigma K_{eq} D_\sigma + \epsilon_\beta D_\beta)\vec{\nabla}^2\{C\} \quad \text{(A25)}$$

Ochoa[45] shows that, by using standard order of magnitude analysis, eqs A23−A25 are satisfied when

$$\frac{\epsilon_\sigma\epsilon_\beta}{a_{\beta\sigma}t^* D_\sigma}\frac{l_\sigma}{}\left(1 + \frac{D_\sigma}{l_\sigma P} + \frac{l_\beta D_\sigma K_{eq}}{l_\sigma D_\beta}\right) \ll K_{eq} + K_{eq}^2\frac{\epsilon_\sigma}{\epsilon_\beta} + \frac{1}{K_{eq}} + \frac{\epsilon_\beta}{K_{eq}^2\epsilon_\sigma} \quad \text{(A26)}$$

$$\frac{\epsilon_\sigma\epsilon_\beta}{a_{\beta\sigma}L^2}\frac{l_\sigma}{}\left(1 + \frac{D_\sigma}{l_\sigma P} + \frac{l_\beta D_\sigma K_{eq}}{l_\sigma D_\beta}\right)\left(1 + \frac{D_\beta}{D_\sigma}\right) \ll K_{eq} + K_{eq}^2\frac{\epsilon_\sigma D_\sigma}{\epsilon_\beta D_\beta} + \frac{1}{K_{eq}} + \frac{D_\beta\epsilon_\beta}{K_{eq}^2 D_\sigma E_\sigma} \quad \text{(A27)}$$

where t^* is the characteristic time and $a_{\beta\sigma}$ is the interfacial area between the β and σ phases per unit volume. Equation A26 reduces to $7.3 \times 10^{-7} \ll 5.5$, and eq A27 reduces to $1.2 \times 10^{-12} \ll 8.0$, for the parameters used in the main body of the text; thus both constraints are satisfied. When eqs A23−A25 are satisfied, eq A22 reduces to

$$(\epsilon_\sigma K_{eq} + \epsilon_\beta)\frac{\partial\{C\}}{\partial t} = \vec{\nabla}\cdot\left\{(\epsilon_\sigma K_{eq} D_\sigma + \epsilon_\beta D_\beta)\vec{\nabla}\{C\} + \frac{D_\sigma}{V}\int_{A_{\beta\sigma}} \hat{n}_{\sigma\beta}\tilde{C}_\sigma \, dA + \frac{D_\sigma}{V}\int_{A_{\alpha\sigma}} \hat{n}_{\sigma\alpha}\tilde{C}_\sigma \, dA + \frac{D_\beta}{V}\int_{A_{\beta\sigma}} \hat{n}_{\beta\sigma}\tilde{C}_\beta \, dA\right\} \quad \text{(A28)}$$

Equation A28 is the one equation model for the current system.

To use eq A28 to predict effective diffusivities, the local spatial deviation concentrations must be known. To solve for these variables, the procedure of Nozad et al.[75] and Crapiste et al.[81] is followed. Applying Gray's decomposition (eq A13) to eq 2 results in

$$\frac{\partial\langle C_\sigma\rangle^\sigma}{\partial t} - \vec{\nabla}\cdot(D_\sigma\vec{\nabla}\langle C_\sigma\rangle^\sigma) = -\left[\frac{\partial\tilde{C}_\sigma}{\partial t} - \vec{\nabla}\cdot(D_\sigma\vec{\nabla}\tilde{C}_\sigma)\right] \quad \text{(A29)}$$

Taking the intrinsic phase average of this equation leads to

$$\left\langle\frac{\partial\langle C_\sigma\rangle^\sigma}{\partial t} - \vec{\nabla}\cdot(D_\sigma\vec{\nabla}\langle C_\sigma\rangle^\sigma)\right\rangle^\sigma = -\left\langle\frac{\partial\tilde{C}_\sigma}{\partial t} - \vec{\nabla}\cdot(D_\sigma\vec{\nabla}\tilde{C}_\sigma)\right\rangle^\sigma \quad \text{(A30)}$$

Following the treatment of Ochoa,[45] when the length constraints are satisfied, eq A30 can be expressed as

$$\frac{\partial\langle C_\sigma\rangle^\sigma}{\partial t} - \vec{\nabla}\cdot(D_\sigma\vec{\nabla}\langle C_\sigma\rangle^\sigma) = -\left\langle\frac{\partial\tilde{C}_\sigma}{\partial t} - \vec{\nabla}\cdot(D_\sigma\vec{\nabla}\tilde{C}_\sigma)\right\rangle^\sigma \quad \text{(A31)}$$

Substitution of eq A29 into eq A31 yields

$$\frac{\partial\tilde{C}_\sigma}{\partial t} - \vec{\nabla}\cdot(D_\sigma\vec{\nabla}\tilde{C}_\sigma) = \left\langle\frac{\partial\tilde{C}_\sigma}{\partial t} - \vec{\nabla}(D_\sigma\vec{\nabla}\tilde{C}_\sigma)\right\rangle^\sigma \quad \text{(A32)}$$

It is possible to neglect the transient terms in eq A32 if the following constraint is satisfied:

$$\frac{D_\sigma t^*}{l_\sigma^2} \gg 1 \quad \text{(A33)}$$

The left-hand side of eq A33 is 1.5×10^5, thus satisfying the constraint. If we neglect variations in D_σ and also impose the constraint that

$$\vec{\nabla}D_\sigma\cdot\vec{\nabla}\tilde{C}_\sigma \ll D_\sigma\vec{\nabla}^2\tilde{C}_\sigma \quad \text{(A34)}$$

then eq A32 becomes

$$\vec{\nabla}^2\tilde{C}_\sigma = \frac{1}{V_\sigma}\int_{V_\sigma}\vec{\nabla}^2\tilde{C}_\sigma \, dV \quad \text{(A35)}$$

with an analogous equation for the β phase.

Using the definitions of the local spatial deviation concentrations and the macroscopic spatial deviation

concentrations, the first three boundary conditions can be written as

$$\text{BC1:} \quad -\hat{n}_{\beta\sigma}\cdot D_\beta\vec{\nabla}\{C\} - \hat{n}_{\beta\sigma}\cdot D_\beta\vec{\nabla}\tilde{C}_\beta - \hat{n}_{\beta\sigma}\cdot D_\beta\vec{\nabla}\tilde{C}_\beta = -K_{eq}\hat{n}_{\beta\sigma}\cdot D_\sigma\vec{\nabla}\{C\} - \hat{n}_{\beta\sigma}\cdot D_\sigma\vec{\nabla}\tilde{C}_\sigma - \hat{n}_{\beta\sigma}\cdot D_\sigma\vec{\nabla}\tilde{C}_\sigma \quad \text{at } A_{\beta\sigma} \tag{A36}$$

$$\text{BC2:} \quad -K_{eq}\hat{n}_{\sigma\beta}\cdot D_\sigma\vec{\nabla}\{C\} - \hat{n}_{\sigma\beta}\cdot D_\sigma\vec{\nabla}\hat{C}_\sigma - \hat{n}_{\sigma\beta}\cdot D_\sigma\vec{\nabla}\tilde{C}_\sigma = P\{\hat{C}_\sigma + \tilde{C}_\sigma - K_{eq}(\hat{C}_\beta + \tilde{C}_\beta)\} \quad \text{at } A_{\beta\sigma} \tag{A37}$$

$$\text{BC3:} \quad K_{eq}\hat{n}_{\alpha\sigma}\cdot D_\sigma\vec{\nabla}\{C\} + \hat{n}_{\alpha\sigma}\cdot D_\sigma\nabla\hat{C}_\sigma + \hat{n}_{\alpha\sigma}\cdot D_\sigma\vec{\nabla}\tilde{C}_\sigma = 0 \quad \text{at } A_{\alpha\sigma} \tag{A38}$$

These three boundary conditions can be simplified by using the fact that the local spatial deviation concentrations are large compared to the macroscopic spatial deviation concentrations

$$\tilde{C}_\sigma \gg \hat{C}_\sigma \; \tilde{C}_\beta \gg \hat{C}_\beta \tag{A39}$$

Ochoa[45] derives these constraints and points out that they were already imposed in order to obtain the one-equation model. The use of the following definitions also simplifies the boundary conditions

$$\bar{\kappa} = \frac{D_\sigma K_{eq}}{D_\beta} \quad \alpha_\sigma' = \frac{D_\sigma}{P} \quad \tilde{b}_\sigma = \frac{\tilde{C}_\sigma}{K_{eq}} \tag{A40}$$

Using eqs A39−A40, the first three boundary conditions simplify to

$$\text{BC 1:} \quad n_{\beta\sigma}\cdot\vec{\nabla}\tilde{C}_\beta = \bar{\kappa}\hat{n}_{\beta\sigma}\cdot\vec{\nabla}\tilde{b}_\sigma + (\bar{\kappa} - 1)\hat{n}_{\beta\sigma}\cdot\vec{\nabla}\{C\} \quad \text{at } A_{\beta\sigma} \tag{A41}$$

$$\text{BC 2:} \quad \tilde{b}_\sigma - \tilde{C}_\beta = -\alpha_\sigma'\hat{n}_{\sigma\beta}\cdot\nabla\tilde{b}_\sigma - \alpha_\sigma'\hat{n}_{\sigma\beta}\cdot\vec{\nabla}\{C\} \quad \text{at } A_{\beta\sigma} \tag{A42}$$

$$\text{BC 3:} \quad \hat{n}_{\alpha\sigma}\cdot\vec{\nabla}\{C\} + \hat{n}_{\alpha\sigma}\cdot\nabla\tilde{b}_\sigma = 0 \quad \text{at } A_{\alpha\sigma} \tag{A43}$$

The fourth boundary condition becomes

$$\text{BC 4a:} \quad \tilde{C}_\beta = f(\vec{r}) \quad \text{at } A_{\beta e} \tag{A44}$$

$$\text{BC 4b:} \quad \tilde{b}_\sigma = g(\vec{r}) \quad \text{at } A_{\sigma e} \tag{A45}$$

Ochoa,[45] Ryan et al.,[72] and Nozad et al.[75] have shown that this closure problem needs to be solved only in a representative region, and therefore, the boundary conditions for the entrances and exits of the macroscopic system can be abandoned and replaced by periodic boundary conditions given by

$$\text{BC 4a:} \quad \tilde{C}_\beta(\vec{r}) = \tilde{C}_\beta(\vec{r} + \vec{l}_i) \quad i = 1, 2, 3 \tag{A46}$$

$$\text{BC 4b:} \quad \tilde{b}_\sigma(\vec{r}) = \tilde{b}_\sigma(\vec{r} + \vec{l}_i) \quad i = 1, 2, 3 \tag{A47}$$

Ochoa[45] shows that without introducing new restrictions and by imposing the periodic boundary conditions, eq A35 and the comparable equation for the σ phase can be written as

$$\vec{\nabla}^2\tilde{C}_\beta = 0 \quad \text{in } V_\beta \tag{A48}$$

$$\vec{\nabla}^2\tilde{b}_\sigma = 0 \quad \text{in } V_\sigma \tag{A49}$$

The following solutions are proposed for spatially periodic porous media[75]

$$\tilde{C}_\beta = \vec{f}\cdot\vec{\nabla}\{C\} \tag{A50}$$

$$\tilde{b}_\sigma = \vec{g}\cdot\vec{\nabla}\{C\} \tag{A51}$$

The closure problem can now be proposed as

$$\vec{\nabla}^2\vec{f} = 0 \quad \text{in } V_\beta \tag{A52}$$

$$\vec{\nabla}^2\vec{g} = 0 \quad \text{in } V_\sigma \tag{A53}$$

$$\text{BC 1:} \quad \hat{n}_{\beta\sigma}\cdot\nabla\vec{f} = \bar{\kappa}\hat{n}_{\beta\sigma}\cdot\nabla\vec{g} + (\bar{\kappa} - 1)\hat{n}_{\beta\sigma} \quad \text{at } A_{\beta\sigma} \tag{A54}$$

$$\text{BC 2:} \quad -\hat{n}_{\sigma\beta} - \hat{n}_{\sigma\beta}\cdot\vec{\nabla}\vec{g} = \frac{1}{\alpha_\sigma'}(\vec{g} - \vec{f}) \quad \text{at } A_{\beta\sigma} \tag{A55}$$

$$\text{BC 3:} \quad \hat{n}_{\alpha\sigma}\cdot\vec{\nabla}\vec{g} + \hat{n}_{\alpha\sigma} = 0 \quad \text{at } A_{\alpha\sigma} \tag{A56}$$

$$\text{BC 4a:} \quad \vec{f}(\vec{r}) = \vec{f}(\vec{r} + \vec{l}_i) \quad i = 1, 2, 3 \tag{A57}$$

$$\text{BC 4b:} \quad \vec{g}(\vec{r}) = \vec{g}(\vec{r} + \vec{l}_i) \quad i = 1, 2, 3 \tag{A58}$$

It is also required that the following averages be zero

$$\frac{1}{V_\beta}\int_{V_\beta}\vec{f}\,dV = 0 \qquad \frac{1}{V_\sigma}\int_{V_\sigma}\vec{g}\,dV = 0 \tag{A59}$$

Returning to the one-equation model, eq A28, substitution of eqs A50 and A51 yields

$$\frac{\partial\{C\}}{\partial t} = \vec{\vec{D}}_{eff}:\vec{\nabla}\vec{\nabla}\{C\} \tag{A60}$$

For isotropic systems the effective diffusivity tensor reduces to a scalar, and $\vec{\nabla}\vec{\nabla}\{C\}$ reduces to $\vec{\nabla}^2\{C\}$. Therefore, the nondimensional effective diffusivity tensor is given by

$$\vec{\vec{D}}^* = \frac{\vec{\vec{D}}_{eff}}{D_\beta}(\epsilon_\sigma K_{eq} + \epsilon_\beta) = (\epsilon_\sigma\bar{\kappa} + \epsilon_\beta)\vec{\vec{I}} + \frac{\bar{\kappa}}{V}\int_{A_{\beta\sigma}}\frac{1}{2}(\hat{n}_{\sigma\beta}\vec{g} + \vec{g}\hat{n}_{\sigma\beta})\,dA + \frac{\bar{\kappa}}{V}\int_{A_{\alpha\sigma}}\frac{1}{2}(\hat{n}_{\sigma\alpha}\vec{g} + \vec{g}\hat{n}_{\sigma\alpha})\,dA + \frac{1}{V}\int_{A_{\beta\sigma}}\frac{1}{2}(\hat{n}_{\beta\sigma}\vec{f} + \vec{f}\hat{n}_{\beta\sigma})\,dA \tag{A61}$$

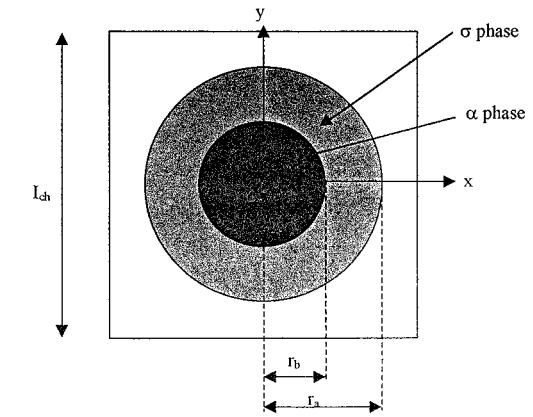

(a) Original unit cell for the Pluronic system.

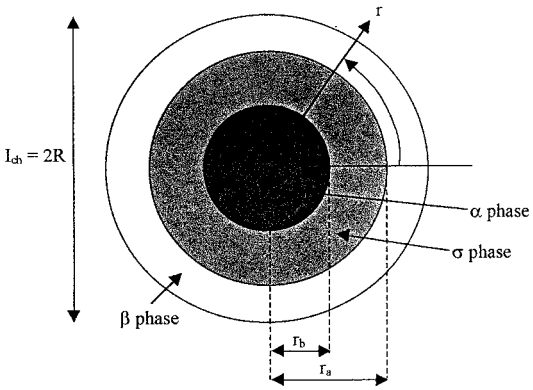

(b) Pluronic unit cell with modification suggested by Chang (1982).

Figure 10. Unit cells for the Pluronic system: (a) original square unit cell; (b) circular unit cell modified from that suggested by Chang.[82]

Now, if one can obtain a solution to the closure problem, the effective diffusivity can be predicted. It should be noted that the difference between eq A61 and previous work[45] is the addition of the third term on the right-hand side of eq A61.

The closure problem must be solved in a representative region or unit cell, and this development closely follows that of Ochoa.[45] The unit cell most appropriate for the Pluronic copolymer liquid crystal system is a square unit cell containing a circular α phase surrounded by a circular σ phase surrounded by the β phase (Figure 10a). To solve this problem analytically, Chang[82] suggested modifying the square unit cell to become a circular unit cell (Figure 10b). As shown in Figure 10b, r_a is the radius of the $\beta-\sigma$ interface, r_b is the radius of the $\sigma-\alpha$ interface, and $R = I_{ch}/2$ is the radius of the circular unit cell. The unit normal vector in the $r$direction can be expressed in terms of the Cartesian unit vectors as follows

$$\hat{e}_r = \hat{\imath}\cos\theta + \hat{\jmath}\sin\theta \tag{A62}$$

Defining the following dimensionless variables

$$\vec{F} = \frac{2\vec{f}}{I_{ch}} \quad \vec{G} = \frac{2\vec{g}}{I_{ch}} \quad \xi = \frac{2r}{I_{ch}} \quad \alpha_\sigma = \frac{2\alpha_\sigma'}{I_{ch}} \tag{A63}$$

the dimensionless boundary value problem becomes

$$\frac{1}{\xi}\frac{\partial}{\partial\xi}\left(\xi\frac{\partial F_x}{\partial\xi}\right) + \frac{1}{\xi^2}\frac{\partial^2 F_x}{\partial\theta^2} = 0 \quad \text{in } (1-\epsilon_\beta)^{1/2} \le \xi \le 1 \tag{A64}$$

$$\frac{1}{\xi}\frac{\partial}{\partial\xi}\left(\xi\frac{\partial G_x}{\partial\xi}\right) + \frac{1}{\xi^2}\frac{\partial^2 G_x}{\partial\theta^2} = 0 \quad \text{in } \epsilon_\alpha^{1/2} \le \xi \le (1-\epsilon_\beta)^{1/2} \tag{A65}$$

$$\text{BC 1:} \quad \frac{\partial F_x}{\partial\xi} = \bar{\kappa}\frac{\partial G_x}{\partial\xi} + \cos\theta(\bar{\kappa}-1) \quad \text{at } \xi = (1-\epsilon_\beta)^{1/2} \tag{A66}$$

$$\text{BC 2:} \quad -\cos\theta - \frac{\partial G_x}{\partial\xi} = \frac{1}{\alpha_\sigma}(G_x - F_x) \quad \text{at } \xi = (1-\epsilon_\beta)^{1/2} \tag{A67}$$

$$\text{BC 3:} \quad \frac{\partial G_x}{\partial\xi} + \cos\theta = 0 \quad \text{at } \xi = \epsilon_\alpha^{1/2} \tag{A68}$$

$$\text{BC 4a:} \quad F_x = 0 \quad \text{at } \xi = 1 \tag{A69}$$

$$\text{BC 4b:} \quad G_x \text{ is finite} \quad \text{at } \epsilon_\alpha^{1/2} \le \xi \le (1-\epsilon_\beta)^{1/2} \tag{A70}$$

Equations A64 and A65 can be solved by the separation of variables technique to give

$$\vec{F} = C_{21}(\xi^{-1} - \xi)(\hat{\imath}\cos\theta + \hat{\jmath}\sin\theta) \tag{A71}$$

$$\vec{G} = C_{51}(\xi^{-1} + C_3\xi)(\hat{\imath}\cos\theta + \hat{\jmath}\sin\theta) \tag{A72}$$

where $C_{2\gamma}$, $C_{5\mu}$, and C_3 are

$$C_{21} = \frac{-2\epsilon_p + (\bar{\kappa}+1)\epsilon_\sigma - \alpha_\sigma\epsilon_p^{-1/2}\epsilon_\sigma}{-4 + 2\epsilon_\beta + (\bar{\kappa}+1)\epsilon_\sigma + (1-\bar{\kappa})\epsilon_p^{-1}\epsilon_\sigma - \alpha_\sigma\epsilon_\sigma\epsilon_p^{-3/2}(2-\epsilon_\beta)} \tag{A73}$$

$$C_{51} = \frac{-2\epsilon_\alpha}{-4 + 2\epsilon_\beta + (\bar{\kappa}+1)\epsilon_\sigma + (1-\bar{\kappa})\epsilon_p^{-1}\epsilon_\sigma - \alpha_\sigma\epsilon_\sigma\epsilon_p^{-3/2}(2-\epsilon_\beta)} \tag{A74}$$

$$C_3 = \frac{-2\epsilon_p + (\bar{\kappa}+1)\epsilon_\sigma + (1-\bar{\kappa})\epsilon_p^{-1}\epsilon_\sigma - \alpha_\sigma\epsilon_\sigma\epsilon_p^{-3/2}(2-\epsilon_\beta)}{2\epsilon_\alpha} \tag{A75}$$

where $\epsilon_p = \epsilon_\alpha + \epsilon_\sigma$.

Now, eqs A71 and A72 need to be substituted into eq A61 to solve for the effective diffusivity. It should be noted again that the current analysis is a two-dimensional analysis, and some changes have to be made in eq A61 to account for this. The volumes in eq A61 have to be changed to areas, and the area integrals need to be changed to line integrals. Making these changes and the above substitutions leads to eq 8 for the effective

diffusion coefficient given in the text. Additional details are given by Hadden.[83]

References and Notes

(1) Wu, G.; Chu, B.; Schneider, D. K. *J. Phys. Chem.* **1995**, *99*, 5094.
(2) Wu, C.; Liu, T.; Chu, B.; Schneider, D.; Graziano, V. *Macromolecules* **1997**, *30*, 4574.
(3) Rill, R. L.; Locke, B. R.; Liu, Y.; Van Winkle, D. H. *Proc. Natl. Acad. Sci. U.S.A.* **1998**, *95*, 1534.
(4) Rill, R. L.; Liu, Y.; Van Winkle, D. H.; Locke, B. R. *J. Chromatogr.* **1998**, *A817*, 287.
(5) Rill, R. L.; Ramey, B. A.; Van Winkle, D. H.; Locke, B. R. *Chromatographia* **1999** (Suppl. I), *49*, S65.
(6) Yiu, Y.; Locke, B. R.; Van Winkle, D. H.; Rill, R. L. *J. Chromatogr.* **1998**, *A817*, 367.
(7) Zhao, D.; Feng, J.; Hou, Q.; Melosh, N.; Gredirckson, G. H.; Chmelka, B. F.; Stucky, G. D. *Science* **1998**, *279*, 548.
(8) Linse, P. *J. Phys. Chem.* **1993**, *97*, 13896.
(9) Wanka, G.; Hoffman, H.; Ulbricht, W. *Macromolecules* **1994**, *27*, 4145.
(10) Linse, P.; Malmsten, M. *Macromolecules* **1992**, *25*, 5434.
(11) Malmsten, M.; Lindman, B. *Macromolecules* **1992**, *25*, 5440.
(12) Zhou, Z.; Chu, B. *J. Colloid Interface Sci.* **1988**, *126*, 171.
(13) Brown, W.; Schillen, K.; Hvidt, S. *J. Phys. Chem.* **1992**, *96*, 038.
(14) Prud'homme, R. K.; Wu, G.; Schneider, D. K. *Langmuir* **1996**, *12*, 4651.
(15) Mortensen, K.; Talmon, Y. *Macromolecules* **1995**, *28*, 8829.
(16) Hvidt, S.; Jorgensen, E. B.; Brown, W.; Schillen, K. *J. Phys. Chem.* **1994**, *98*, 12320.
(17) Malmsten, M.; Lindman, B. *Macromolecules* **1992**, *25*, 5446.
(18) Mortensen, K.; Brown, W.; Norden, B. *Phys. Rev. Lett.* **1992**, *68*, 2340.
(19) Chrambach, A. *The Practice of Quantitative Gel Electrophoresis*; VCH: Weinheim, 1985.
(20) Ramey, B. A. Master of Science Thesis, Florida State University, Tallahassee, 1998.
(21) Doi, M.; Edwards, S. F. *The Theory of Polymer Dynamics*; Oxford University Press: Oxford, 1986.
(22) De Gennes, P.-G. *Scaling Concepts in Polymer Physics*; Cornell University Press: Ithaca, NY, 1979.
(23) Baumgartner, A.; Muthukumar, M. *Adv. Chem. Phys.* **1996**, *94*, 625.
(24) Rouse, P. E. *J. Chem. Phys.* **1953**, *21*, 1272.
(25) Zimm, B. H. *J. Chem. Phys.* **1956**, *24*, 269.
(26) Brochard, F.; de Gennes, P. G. *J. Chem. Phys.* **1977**, *67*, 52.
(27) De Gennes, P. G. *Macromolecules* **1976**, *9*, 587.
(28) Fixman, M *J. Chem. Phys.* **1965**, *42*, 3831.
(29) Phillies, G. D. J. *J. Phys. Chem.* **1989**, *93*, 5029.
(30) Mackie, J. S.; Meares, P. *Proc. R. Soc. London, Ser. A* **1955**, *232*, 498.
(31) Vrentas, J. S.; Duda, J. L. *J. Polym. Sci., Polym. Phys. Ed.* **1977**, *15*, 403.
(32) Vrentas, J. S.; Duda, J. L. *J. Polym. Sci., Polym. Phys. Ed.* **1977**, *15*, 417.
(33) Vrentas, J. S.; Duda, J. L. *J. Polym. Sci., Polym. Phys. Ed.* **1977**, *15*, 441.
(34) Johansson, L.; Lofroth, J.-E. *J. Chem. Phys.* **1993**, *98*, 7471.
(35) Johansson, L.; Elvingson, C.; Lofroth, J. E. *Macromolecules* **1991**, *24*, 6024.
(36) Johansson, L.; Skantze, U.; Lofroth, J.-E. *Macromolecules* **1991**, *24*, 6019.
(37) Whitaker, S. *The Method of Volume Averaging*; Kluwer Academic Publishers: Dordrecht, 1998.
(38) Hahn, E. L. *Phys. Rev.* **1950**, *80*, 580.
(39) Carr, H. Y.; Purcell, E. M. *Phys. Rev.* **1954**, *94*, 630.
(40) Stejskal, E. O.; Tanner, J. E. *J. Chem. Phys.* **1965**, *42*, 288.
(41) Tanner, J. E. *J. Chem. Phys.* **1970**, *52*, 2523.
(42) Wu, D.; Chen, A.; Johnson, C. S. *J. Magn. Reson., Ser. A* **1995**, *115*, 123.
(43) Gibbs, S. J.; Johnson, C. S. *J. Magn. Reson.* **1991**, *93*, 395.
(44) Whitaker, S. *AIChE J.* **1967**, *13*, 420.
(45) Ochoa, J. A. Ph.D. Dissertation, University of California Davis, 1988.
(46) Landau, L. D.; Lifshitz, E. M. *Statistical Physics*; Addison-Wesley: Reading, MA, 1958.
(47) Adler, P. M. *Porous Media, Geometry and Transports*; Butterworth-Heinemann: Boston, 1992.
(48) Yang, X.; Sanghvi, Y. S.; Gao, X. *J. Biomol. NMR* **1997**, *10*, 383.
(49) Kratky, O.; Porod, G. *Recl. Trav. Chim.* **1949**, *68*, 1106.
(50) Grossman, P. D. Free-Solution Capillary Electrophoresis. In *Capillary Electrophoresis, Theory and Practice*; Grossman, P. D., Colburn, J. C., Eds.; Academic Press: San Diego, 1992; p 111.
(51) Stellwagen, N. C.; Gelfi, C.; Righetti, P. G. *Biopolymers* **1997**, *42*, 687.
(52) Volkel, A. R.; Noolandi, J. *Macromolecules* **1995**, *28*, 8182.
(53) Volkel, A. R.; Noolandi, J. *J. Chem. Phys.* **1995**, *102*, 5506.
(54) Muthukumar, M. *Macromol. Theory Simul.* **1994**, *3*, 61.
(55) Ogston, A. G. *Trans. Faraday Soc.* **1958**, *54*, 1754.
(56) Morris, C. J. O. R. *Protides Biol. Fluids* **1966**, *14*, 543.
(57) Rodbard, D.; Chrambach, A. *Proc. Natl. Acad. Sci. U.S.A.* **1970**, *65*, 970.
(58) Locke, B. R. *Ind. Eng. Chem. Res.* **1998**, *36*, 615.
(59) Locke, B. R.; Trinh, S. H. *Electrophoresis* **1999**, *20*, 3331.
(60) Muthukumar, M.; Baumgartner, A. *Macromolecules* **1989**, *22*, 1937.
(61) Melenkevitz, J.; Muthukumar, M. *Chemtracts: Macromol. Chem.* **1990**, *1*, 171.
(62) Cukier, R. I. *Macromolecules* **1984**, *17*, 252.
(63) Phillies, G. D. J. *Macromolecules* **1986**, *19*, 2367.
(64) Phillies, G. D. J. *Macromolecules* **1987**, *20*, 558.
(65) Phillies, G. D. J. *Macromolecules* **1988**, *21*, 3101.
(66) Lin, T. H.; Phillies, G. D. J. *J. Colloid Interface Sci.* **1984**, *100*, 82.
(67) Radko, S. P.; Chrambach, A. *Macromolecules* **1999**, *32*, 2617.
(68) Gibbs, S. J.; Johnson, C. S. *Macromolecules* **1991**, *24*, 6110.
(69) Maxwell, J. C. *A Treatise on Electricity and Magnetism*, 3rd ed.; Dover Publications: New York, 1981; Vol. 1.
(70) Archie, G. E. *Trans. Am. Inst. Mining Eng.* **1942**, *146*, 54.
(71) Perrins, W. T.; McKenzie, D. R.; McPhedran, R. C. *Proc. R. Soc. London, Ser. A* **1979**, *369*, 207.
(72) Ryan, D. J.; Carbonell, R. G.; Whitaker, S. *AIChE Symp. Ser.* **1981**, *71*, 46.
(73) Kim, J. H.; Ochoa, J. A.; Whitaker, S. *Transport Porous Media* **1987**, *2*, 327.
(74) Wakao, N.; Smith, J. M. *Chem. Eng. Sci.* **1962**, *17*, 825.
(75) Nozad, I.; Carbonell, R. G.; Whitaker, S. *Chem. Eng. Sci.* **1985**, *40*, 843.
(76) Carbonell, R. G.; Whitaker, S. Heat and Mass Transfer in Porous Media. In *Fundamentals of Transport Phenomena in Porous Media*, NATO ASI Series, Series E: Applied Sciences, No. 82; Bear, J., Corapcioplu, M. Y., Eds.; Marinus Nijhoff Publishers: Dordrecht, 1984; p 121.
(77) Anderson, T. B.; Jackson, R. *Ind. Eng. Chem. Fundam.* **1967**, *6*, 527.
(78) Slattery, J. *AIChE J.* **1967**, *13*, 1066.
(79) Gray, W. G. *Chem. Eng. Sci.* **1975**, *30*, 229.
(80) Whitaker, S. *Chem. Eng. Sci.* **1986**, *41*, 2029.
(81) Crapiste, G. H.; Rotstein, E.; Whitaker, S. *Chem. Eng. Sci.* **1986**, *41*, 227.
(82) Chang, H.-C. *Chem. Eng. Commun.* **1982**, *15*, 83.
(83) Hadden, D. A. Master of Science Thesis, Florida State University, Tallahassee, 1999.

MA9915071